nature medicine

A critical developmental switch defines the kinetics of kidney cyst formation after loss of *Pkd1*

Klaus Piontek[1], Luis F Menezes[1], Miguel A Garcia-Gonzalez[1], David L Huso[2,3] & Gregory G Germino[1,4]

Autosomal dominant polycystic kidney disease is an important cause of end-stage renal disease, for which there is no proven therapy[1]. Mutations in *PKD1* (the gene encoding polycystin-1) are the principal cause of this disease. The disease begins *in utero*[2] and is slowly progressive, but it is not known whether cystogenesis is an ongoing process during adult life. We now show that inactivation of *Pkd1* in mice before postnatal day 13 results in severely cystic kidneys within 3 weeks, whereas inactivation at day 14 and later results in cysts only after 5 months. We found that cellular proliferation was not appreciably higher in cystic specimens than in age-matched controls, but the abrupt change in response to *Pkd1* inactivation corresponded to a previously unrecognized brake point during renal growth and significant changes in gene expression. These findings suggest that the effects of *Pkd1* inactivation are defined by a developmental switch that signals the end of the terminal renal maturation process. Our studies show that *Pkd1* regulates tubular morphology in both developing and adult kidney, but the pathologic consequences of inactivation are defined by the organ's developmental status. These results have important implications for clinical understanding of the disease and therapeutic approaches.

Autosomal dominant polycystic kidney disease (ADPKD) is characterized by the gradual replacement of renal tubules by cysts, which results in end-stage renal disease in approximately 50% of affected individuals by the sixth decade of life[1]. An unanswered question with important clinical implications is whether cyst initiation is an ongoing process throughout the lifetime of an individual, or whether it is restricted to the period of rapid growth during development and early childhood. A related question is whether *PKD1* is required for maintenance of renal tubular structure in adult kidneys. To address these issues, we induced *Pkd1* inactivation in mice homozygous for a floxed *Pkd1* allele[3] at various time points. Inactivation at postnatal day 2 (P2), a time of ongoing cortical nephrogenesis in the mouse, resulted in grossly enlarged, homogenously cystic kidneys within 2 weeks (**Fig. 1a**). The cortical rim lacked immature or dysplastic elements, indicating that *Pkd1* is not required for initial fate decisions during nephrogenesis, which is consistent with previous studies in mice with homozygous germline *Pkd1* mutations[4]. Using nephron segment–specific markers, we found that cysts originated from all tubular segments (**Fig. 1a** and **Supplementary Fig. 1a** online).

We next determined whether inactivation of *Pkd1* in adult kidneys was sufficient to cause cystic disease by inducing its inactivation in 6-week-old mice (**Fig. 1b,c**). In contrast to the results of inactivation at P2, we found that the kidneys of these mice, 3 months after inactivation of *Pkd1*, appeared normal in gross and histopathologic analyses, despite the fact that we had achieved *Pkd1* inactivation with >50% efficiency (**Fig. 1d**). By 6 months after inactivation, however, kidneys were grossly cystic, with cysts derived from all nephron segments (**Fig. 1c,e** and **Supplementary Fig. 1b**). Notably, the proliferation rate of cystic epithelia (as measured by Ki-67 staining) seemed to be slightly higher than that of renal tubular epithelia in age-matched normal control samples, but the difference was not significant, possibly because of the relatively small sample size (**Fig. 1f** and **Table 1a**). Hypothesizing that a difference in growth rate between young and adult mice might be the reason for our observations, we determined the effects of *Pkd1* inactivation in adolescent mice (~3 weeks old). We achieved rates of *Pkd1* inactivation in the mice at this age that were similar to those in adults, and we also obtained identical results to those observed in adults. Kidneys of treated mice did not show cystic change until ~5 months after inactivation (data not shown). These results confirmed that the *Pkd1* gene is essential for maintenance of normal tubular structure in adult tissues but, notably, revealed the very different disease progressions that result from early versus late *Pkd1* inactivation.

To define the crucial time interval for the differences between the early- and late-inactivation phenotypes and determine the factors responsible for these differences, we induced inactivation at various time points between P2 and P21 with the same protocol used for the P2 inductions (**Supplementary Table 1** online). All induced $Pkd1^{cond/cond}$ mice P12 or younger developed severe cystic disease within 3 weeks, whereas all control mice were free of cysts at the same time point (**Fig. 2a** and data not shown). Of note, mice induced at ages between P14 and P21, the kidneys of which appeared normal in gross and microscopic examinations 3 months after induction (**Fig. 2a** and data not shown), reproducibly had late-onset cystic disease (that is, onset of disease by 6 months after Cre induction; data not shown)

[1]Division of Nephrology, Department of Medicine, Johns Hopkins University School of Medicine, Ross 958, 720 Rutland Avenue, Baltimore, Maryland 21205, USA. [2]Department of Molecular and Comparative Pathobiology, Johns Hopkins University School of Medicine, Suite 851 Broadway Research Building, 735 North Broadway, Baltimore, Maryland 21205, USA. [3]Sidney Kimmel Comprehensive Cancer Center and [4]Department of Molecular Biology and Genetics, Johns Hopkins University School of Medicine, Baltimore, Maryland 21205, USA. Correspondence should be addressed to G.G.G. (ggermino@jhmi.edu).

Received 21 May; accepted 1 October; published online 28 October 2007; doi:10.1038/nm1675

identical to that seen in mice with Cre expression induced later in life (**Fig. 1b**,**c**). In contrast, the livers of the mice induced between P14 and P21 were cystic at both early and later time points. P13 induction resulted in an intermediate phenotype; all mice developed renal cysts within 3 weeks, but the number was variable and reduced compared to mice induced at P12.

In our search for possible explanations of the disparate temporal responses to *Pkd1* inactivation, we excluded trivial explanations based on differences in the pattern or frequency of the gene's inactivation. To confirm the efficacy of our inactivation protocol, we examined the pattern of β-galactosidase staining in the kidneys upon Cre recombinase–mediated activation of the *ROSA26R* reporter transgene at P12 and P14 and found that the staining was similar whether activation occurred at P12 or P14 (**Fig. 2b**). Southern blotting analysis of kidney samples from Cre-induced mice at P12 and P14 revealed that we had achieved similar frequencies of *Pkd1* deletion at these two ages (**Fig. 2c**). In sum, these studies identified a crucial two-day interval that defines the kidney's response to *Pkd1* inactivation.

Increased cellular proliferation and apoptosis have previously been described as primary processes involved in the pathogenesis of ADPKD[5–7]. We therefore stained specimens of littermate-control and cystic mice induced at P7–P12 for markers of these processes

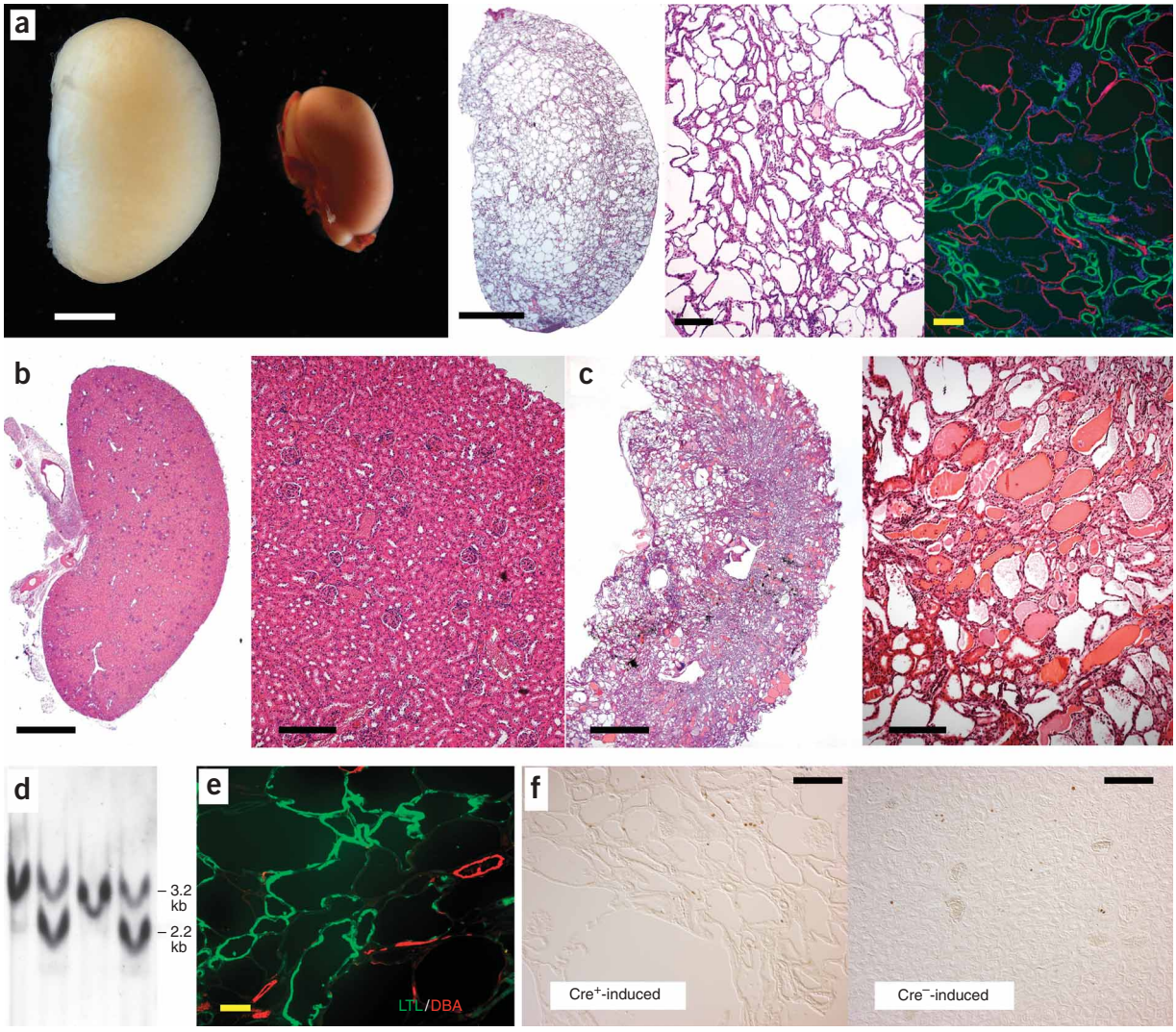

Figure 1 Time of inactivation determines renal response to acquired *Pkd1* loss. (**a**) Early inactivation of *Pkd1* results in rapidly progressive renal cystic disease. Shown are P19 kidneys of *Pkd1*$^{cond/cond}$; tamoxifen-Cre^{+} and *Pkd1*$^{cond/cond}$; tamoxifen-Cre^{-} mice in which *Pkd1* was inactivated on P2. Far left, comparison of gross exam of Cre^{+} (left) and Cre^{-} (right) kidneys. Middle, H&E stains of P19 cystic kidney showing cystic involvement of all nephron segments. Far right, P19 cystic kidney stained with markers for proximal tubule (LTL, green), distal tubule (DBA, red) and nuclei (DAPI, blue), showing that both types of tubules are cystic. Cysts that shared staining for specific markers appeared to be homogeneous in size, consistent with their common time of initiation. Scale bars, 2 mm (left and middle); 100 μm (right). (**b**,**c**) Adult inactivation results in late-onset renal cystic disease. Shown is H&E staining of kidneys harvested 3 months (**b**) or 6 months (**c**) after *Pkd1* inactivation was induced in 6-week-old *Pkd1*$^{cond/cond}$; tamoxifen-Cre^{+} mice. Scale bars, 2 mm (left); 100 μm (right). (**d**) Southern blotting analysis of kidney DNA harvested 3 months after induction of *Pkd1* inactivation in 6-week-old *Pkd1*$^{cond/cond}$; tamoxifen-Cre^{+} mice (lanes 2 and 4) and *Pkd1*$^{cond/cond}$; tamoxifen-Cre^{-} mice (lanes 1 and 3). The *Eco*RI 2.2-kilobase (kb) band is the new fragment resulting from Cre-mediated deletion[3]. (**e**,**f**) LTL (green) and DBA (red) staining of cystic kidneys from *Pkd1*$^{cond/cond}$; tamoxifen-Cre^{+} mice (**e**), and Ki-67 staining of kidney sections from *Pkd1*$^{cond/cond}$; tamoxifen-Cre^{+} (left) and *Pkd1*$^{cond/cond}$; tamoxifen-Cre^{-} mice (right) (**f**), 6 months after Cre induction in 6-week-old mice. Scale bars, 50 μm (**e**); 100 μm (**f**).

Table 1 Proliferation indices of normal and cystic kidneys

(**a**) Cystic versus noncystic adult kidneys

Induced Cre$^+$ (cystic)	Induced Cre$^-$/uninduced (noncystic)
2.73% (3,414/124,967)	1.62% (1,479/91,497)
2.21% (2,224/100,741)	2.56% (2,260/88,130)
4.53% (15,318/337,963)	1.26% (2,468/195,181)
	1.85% (2,743/148,276)
	1.87% (3,390/181,199)

(**b**) Kidneys of Cre$^+$ and Cre$^-$ mice induced at P12 and P14

P12 Cre$^+$	P12 Cre$^-$	P14 Cre$^+$	P14 Cre$^-$
2.75% (3,837/139,343)	2.18% (3,129/143,341)	2.67% (3,037/113,753)	3.16% (3,687/116,544)
1.79% (1,001/55,864)	2.17% (2,054/94,480)	2.75% (3,140/114,241)	2.46% (3,104/126,138)
2.91% (2,256/77,485)	2.67% (3,126/117,041)	3.97% (3,860/97,255)	
		2.37% (2,974/125,411)	

(**c**) Kidneys of wild-type young mice

P14	P16	P19
42.44% (23,996/54,543)	8.6% (7,339/85,282)	7.31% (7,119/97,393)
38.79% (21,901/54,459)	9.07% (6,260/69,010)	7.52% (5,516/73,326)
	14.8% (8,799/59,396)	9.87% (6,361/64,446)

Specimens were stained for Ki-67 and DAPI, and the proliferation rate (%) was calculated as the number of Ki-67–positive cells divided by the total number of DAPI-positive cells that were counted for each sample (ratio in parentheses). Each column identifies the class of specimens that was analyzed, and each row lists the data for a single mouse of each class. (**a**) Proliferation rates in kidneys harvested ~6 months after induction of *Pkd1* inactivation in 6-week-old *Pkd1*$^{cond/cond}$; Cre$^+$ and *Pkd1*$^{cond/cond}$; Cre$^-$ mice. *Pkd1*$^{cond/cond}$; Cre$^-$ mice injected with corn oil served as additional negative controls (uninduced). Any differences were not statistically significant ($P > 0.05$, Mann-Whitney test). (**b**) Proliferation rates in kidneys harvested ~3 weeks after we induced *Pkd1* inactivation in *Pkd1*$^{cond/cond}$; Cre$^+$ and *Pkd1*$^{cond/cond}$; Cre$^-$ mice of the indicated ages. The P12-Cre$^+$ samples were the only ones that were cystic. Any differences were not statistically significant ($P > 0.05$, Kruskal-Wallis test). (**c**) Proliferation rates in kidneys of young mice at the ages indicated. The differences in rates are statistically significant ($P = 0.0482$; Kruskal-Wallis test).

(Ki-67, phospho–histone-3 and caspase-3). Contrary to the published literature, we found few differences in the rate of cell proliferation between control and cystic mice (**Table 1b**). Epithelial cells lining tubules and cysts of control and cystic kidneys stained similarly for Ki-67 and phospho–histone-3, except for small, widely scattered regions of cystic samples that had increased staining (**Fig. 2d** and **Supplementary Fig. 2a** online). Apoptosis was restricted to the renal papilla of wild-type kidneys, whereas cystic specimens had a small number of medullary and cortical cells also undergoing apoptosis (**Supplementary Fig. 2b**). We then examined whether differences in the rates of proliferation or apoptosis in uninduced P12–P19 *Pkd1*$^{cond/cond}$ mice might explain the age-dependent sensitivity to *Pkd1* loss. We found that Ki-67 and phospho–histone-3 expression was similar in the P12 and P14 samples but was markedly different from that observed in the P16 and P19 specimens (**Fig. 2e**, **Table 1c** and **Supplementary Fig. 3a** online), whereas caspase-3 staining was similar at all time points (**Supplementary Fig. 3b**).

Seeking to explain the sudden global decrease in the proliferation rate in the kidney during the P14–P16 interval, we performed microarray analysis of kidney specimens from P11, P12, P14 and P15 control mice. We found few genes differentially expressed between P11 and P12 or between P14 and P15. In contrast, there was a clear change in the expression pattern between the early (P11 and P12) and late (P14 and P15) samples (**Fig. 3** and **Supplementary Table 2** online), including 827 genes whose expression differed significantly between these two stages ($P < 0.001$); of those, 51 had a $\geq$100% increase in at least one animal, and 21 had a $\geq$75% decrease in at least one animal, as compared to mean expression at P11 (**Supplementary Table 3** online). Grouping the results by gene ontological category[8], we found that most of the genes have functional roles in physiological processes, particularly in transporter and catalytic activities (**Supplementary Table 4** online). *In silico* analysis of promoter *cis*-elements showed enrichment for at least one promoter involved in kidney development (*Pea3*; **Supplementary Table 5** online)[9]. These data suggest there is an important developmental switch that is activated in this time frame.

Previous studies have convincingly demonstrated that an increase in cell number must occur to account for the increased surface area of macroscopic cysts in human ADPKD[10]. This outcome has been attributed to the high proliferative rate of renal cystic epithelia[5,6,11,12], and many treatments that are being investigated target this process[5,13,14]. Our data challenge this model. Using two independent markers and a semi-automated system to count large numbers of nuclei from >50 images/specimen, we found that proliferation rates in specimens of adult-onset cystic disease were not appreciably higher than in age-matched control kidney samples. Moreover, we found that the proliferation rate in normal P16 kidneys was several-fold higher than that in adult kidneys, yet inactivation of *Pkd1* at this early time point resulted in the same slow onset of PKD seen in adult mice. These results suggest that defective growth regulation is probably not the primary defect resulting from loss of *Pkd1* and that the relationship between cellular proliferation and cyst formation may be indirect.

There are several potential reasons why our data differ from what has been previously published. First, we used phospho–histone-3 and Ki-67 as markers for proliferation, when most studies of human tissues use proliferating–nuclear cell antigen. The latter may be less reliable and may lead to overestimation of proliferation rates[15]. Second, differences in the antibody source, in sample preparation and in the cell-counting method may also be factors. It should also be noted that most studies of human samples necessarily use late-stage material, in which secondary effects due to chronic renal failure may be superimposed. Acquired cystic disease is thought to be a pre-malignant lesion with increased proliferative potential. Another possibility, which our study cannot address, is that proliferation actually occurs in bursts rather than in a stochastic, random fashion. If proliferation in cysts really occurs in cyclic bursts, it is possible that previous studies happened to catch cysts undergoing bursts of proliferation by chance, whereas ours did not. Finally, we note that a small increase in the rate of proliferation maintained over a prolonged period of time could account for the gradual enlargement seen in human cystic kidneys[11]. However, it is unlikely that this process can explain the abrupt onset of cyst formation seen in our late-onset model.

How might the high proliferation rate in early cystic disease be linked to the disease process? One possibility is that the high proliferation rate is merely a marker for the developmental status of the organ, and the latter is primarily responsible for the enhanced susceptibility to *Pkd1* inactivation. Consistent with this model, the developmental

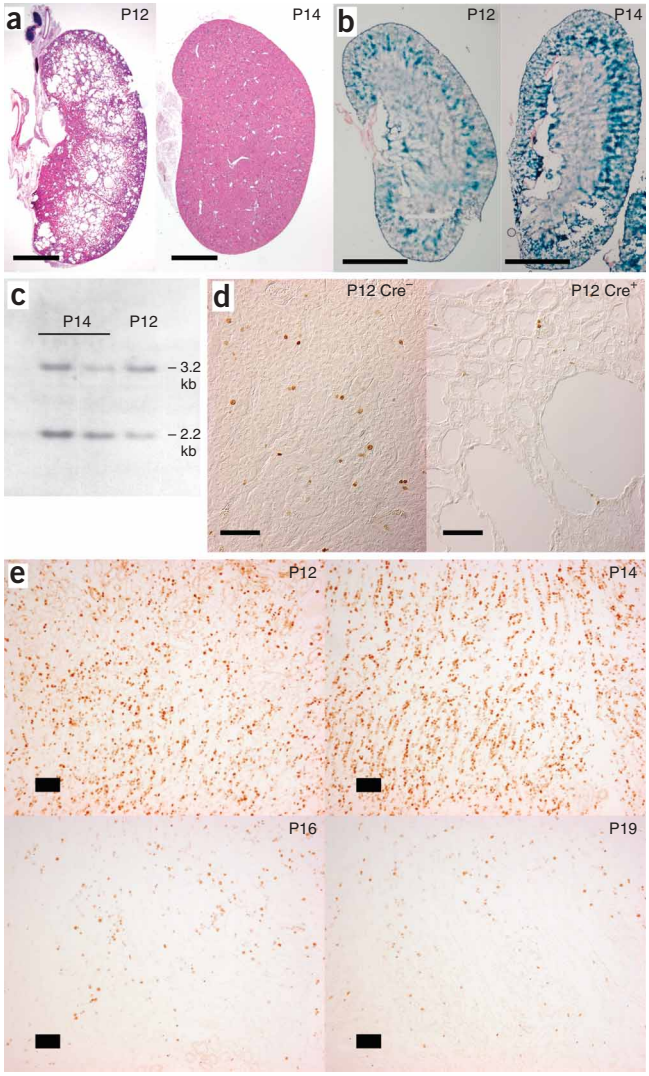

Figure 2 Susceptibility to rapid-onset cystic disease switches off between P12 and P14. (**a**) Kidneys of *Pkd1*$^{cond/cond}$; tamoxifen-Cre^{+} mice induced at P12 were cystic within 3 weeks (left), whereas those of mice induced at P14 remained normal 3 months later (right). Scale bar, 2 mm. (**b**) β-galactosidase staining of kidneys of *ROSA26R* mice 5 d after induction at P12 (left) and P14 (right), showed that the samples have similar patterns and rates of Cre-mediated induction. Scale bar, 2 mm. (**c**) Southern blot of kidney DNA isolated from *Pkd1*$^{cond/cond}$; tamoxifen-Cre^{+} mice harvested 5 d after induction at P12 and P14. (**d**) Ki67-stained sections of *Pkd1*$^{cond/cond}$; tamoxifen-Cre^{+} (left) and *Pkd1*$^{cond/cond}$; tamoxifen-Cre^{-} (right) kidneys 3 weeks after induction at P12. Scale bar, 200 μm. (**e**) Ki67-stained sections of uninduced *Pkd1*$^{cond/cond}$; tamoxifen-Cre^{-}; *ROSA26R*$^{+}$ kidneys harvested on P12–P19. Similar results were obtained for kidneys of uninduced *Pkd1*$^{cond/cond}$; tamoxifen-Cre^{+}; *ROSA26R*$^{+}$ mice (data not shown). Scale bar, 100 μm.

change in the gene expression profile from P12 to P14 preceded the change in proliferation rate and correlated better with the difference between rapid- and slow-onset cystic disease. Alternatively, proliferation may act as an accelerant in the appropriate context. Recent reports suggest that PKD may be the result of aberrant planar polarity within the kidney[16,17]. In zebrafish, planar cell polarity signaling couples cell division and morphogenesis during neurulation[18]. Neuroblasts undergoing proliferation transiently lose their planar orientation but reestablish it as daughter cells reintegrate into the neuroepithelium. Notably, treatment with cell-cycle inhibitors rescues the neural tube defect in zebrafish lacking Vangl2, a conserved component of planar cell polarity signaling[18]. We speculate that renal epithelial cells may undergo a similar process during renal development, and the *Pkd1* gene product, polycystin-1, may have a role in helping cells reorient after cell division. This model may also help to explain the benefits of antiproliferative agents in rodent models of cystic disease, even if proliferation rates are not elevated in these models.

By demonstrating that acquired inactivation of *Pkd1* in adult tissues can result in renal cysts, we provide a mechanistic explanation for the observed acquisition of new cysts during the lifetimes of humans. In contrast to recently reported results in other ADPKD models[19,20], we also show that all nephron segments have the same propensity for forming cysts, which is consistent with the results of previous studies of human samples[11,21–23]. Collectively, these data suggest that cysts derived from proximal tubules may comprise a substantial fraction of the total cyst burden. This may have implications for any therapy whose activity is restricted to cysts derived from distal nephron segments[19].

We also show that the response of the renal epithelium to acquired loss of *Pkd1* is determined by the developmental state of the organ. These data suggest that early acquired inactivation of *Pkd1* may explain the existence of a subset of affected individuals with early, severe ADPKD. The dramatically different response to inactivation in very young mice compared with older mice also suggests that different pathways may be altered in the two groups, which would have important implications for preclinical testing of potential therapies. Most published mouse models of PKD that are used to test therapies, including those for ADPKD, have a relatively rapid onset of disease[5,13,19]. Given the very different rate of progression of disease acquired in adult life, it is unclear whether the approaches used for rapid progression would be equally effective in adult models. The gradual onset of cystic disease and the disease's relatively slow progression in humans suggest that late-onset models, such as the ones identified in this study, may be more predictive of proper treatment of the human condition.

At first glance, the relationship between the developmental status of the kidney and its sensitivity to the effects of *Pkd1* loss seems to be consistent with the 'maturation arrest' hypothesis of cyst formation[24]. This model suggests that cysts are the result of an arrested developmental process that locks cells in an immature state because of a block either in their normal developmental program or in the regenerative program that follows cellular injury. Although our study was not designed to test this hypothesis, we note that there are several aspects of our data that appear inconsistent with the model. For example, we show that fully differentiated, mature renal tubular epithelium can undergo cystic change long after the developmental program has completed. In this case, cysts cannot be the result of a maturation arrest. Although we cannot exclude 'de-differentiation' in response to acquired *Pkd1* loss, there were no signs of renal injury before cyst formation, and cysts formed abruptly and simultaneously throughout the organ. In the case of cyst formation within the first 3 weeks of life, we note that the proliferation rate, which seems to be a very good marker for the incompletely mature state, drops normally in cystic samples. We conclude from these data that kidney cells are particularly susceptible to the loss of *Pkd1* in a developmental context, but we have no data to

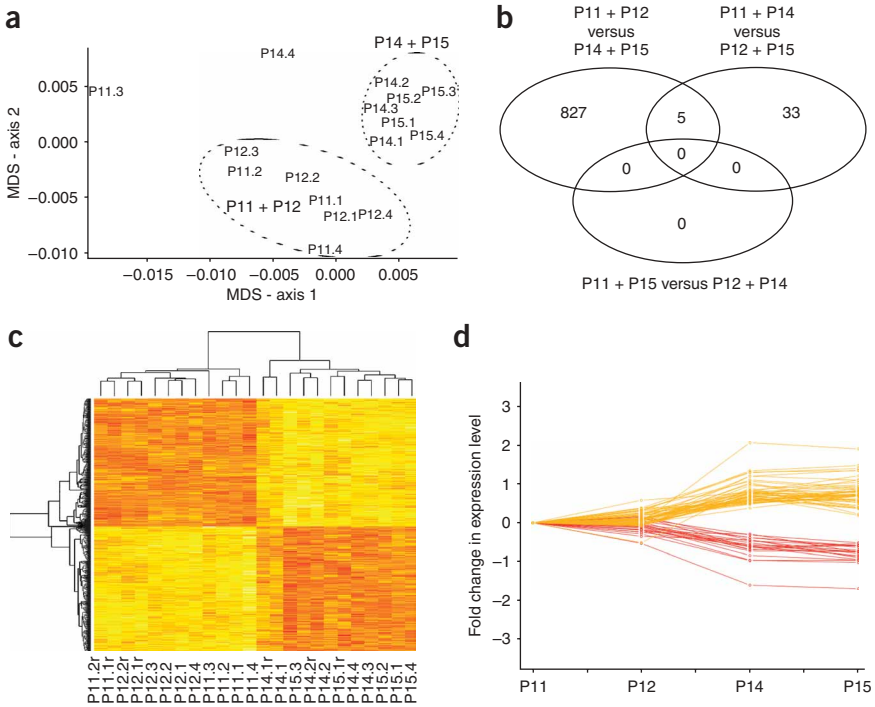

Figure 3 Abrupt brake point in rate of renal proliferation parallels marked changes in gene expression. (**a**) Multidimensional scaling analysis (MDS) of the microarray data revealed that the samples clustered in two groups, separating P11 + P12 (P11 and P12) and P14 + P15 (P14 and P15) kidneys. (**b**) Venn diagram showing that a much larger subset of genes varied between P11 + P12 and P14 + P15 than between other possible groups (*fdr*-adjusted $P < 1 \times 10^{-3}$). (**c**) Heatmap plot of genes ($n = 827$, **Supplementary Table 2**) that varied between the P11 + P12 and P14 + P15 groups, showing a clear switch between the two groups (yellow, greater expression than the mean expression at P11; red, less expression than the mean at P11). (**d**) Plot of fold change in mean expression level at each time point, for genes with *fdr*-adjusted $P < 1 \times 10^{-3}$ and at least a twofold change in expression, in at least one sample, as compared to mean expression at P11 ($n = 72$, **Supplementary Table 3**).

suggest that they are developmentally arrested after *Pkd1* inactivation. Further study will be required to test this hypothesis more thoroughly.

Our data also challenge a prevailing model that depicts the *Pkd1* gene product as a flow sensor on the primary cilia of renal epithelial cells, acting as a means to maintain tubule morphology[25] in the adult kidney. We find it difficult to understand how it could take several months for the alteration of a highly dynamic process such as flow-sensing to result in an observable phenotype. Our conclusions are supported by a recent study that examined the consequences of induced systemic loss of two ciliogenic genes in adults (*Tg737* and *Kif3a*)[26]. Similarly to what we had observed for *Pkd1*, the authors found that the kinetics of cyst formation were dependent on the time at which either gene was inactivated. Given that primary cilia are thought to be the mechanosensitive organelles responsible for dynamic flow-sensing in the kidney, they concluded that loss of flow-sensing in adult kidney is probably not the primary cause of cyst formation in late-onset cystic disease. Neither our study nor the previous one, however, can exclude a role for cilia-based flow-sensing during renal development, given the rapidity with which cysts form after inactivation of *Pkd1*, *Tg737* and *Kif3a* in the immature organ. The functions of cilia and *Pkd1* in the developing kidney may differ from their respective functions in the adult organ, thus accounting for the different rates at which cysts form after their loss. We also cannot exclude a role for the primary cilium as a flow sensor in the adult organ if ciliary signaling has tonic effects rather than dynamic ones on the maintenance of tubular morphology. Yet another possibility is that *Pkd1* and primary cilia are important in establishing and maintaining planar cell polarity that is independent of mechanosensing that is unchanged over time, but the developmental context in which they are lost explains the different phenotypic consequences. Further studies will be required to distinguish between these possibilities.

Finally, these studies have also identified a previously unrecognized brake point during renal growth that corresponds to significant changes in gene expression. The high rate of proliferation, which is universally distributed throughout the kidney, abruptly decreases at ~P15 throughout the organ. These observations suggest that there may be a developmental switch that signals the end of the terminal renal maturation process.

METHODS

***Pkd1*$^{cond/cond}$ mouse lines.** We crossed fifth-generation C57/BL6 *Pkd1*^{cond} mice to fifth-generation C57/BL6 tamoxifen-Cre (B6.Cg-Tg(Cre/Esr1)5Amc/J mice (stock 004682), Jackson Laboratories) and C57/BL6 congenic B6.129S4-*Gt(ROSA)26Sor*^{tm1Sor}/J (stock 003474, Jackson Laboratories) to produce the mice used in these studies. We induced Cre recombinase activity in mice <3 weeks of age by intraperitoneally injecting nursing mothers with either tamoxifen (10 mg/40 g) in corn oil (Sigma-Aldrich) or an equal volume of corn oil alone on two consecutive days. Older mice were induced by direct peritoneal injection with similar doses. Mice were killed by isofluorane treatment and kidneys were processed for DNA and RNA extraction and for histological examination (fixed in 4% paraformaldehyde buffered solution, pH 7.4). DNA was digested with *Eco*RI and probed with a *Bgl2-Eco*RI *Pkd1* fragment located adjacent to the 5′ *loxP* site[3]. All studies were performed using protocols approved by the Johns Hopkins University Animal Care and Use Committee, and mice were housed in pathogen-free facilities accredited by the American Association for the Accreditation of Laboratory Animal Care.

Immunohistochemistry and immunofluorescence. Kidneys and livers from neonate and adult animals were collected and immediately fixed in 4% paraformaldehyde at 4 °C overnight. To remove excess paraformaldehyde, we washed samples in water for 2 h, dehydrated them in 50% ethanol for 2 h and then 70% ethanol for 2 h, and stored them at room temperature in 70% ethanol. After rehydration in water for 2 h, we dehydrated all samples in a graded alcohol series and embedded them in paraffin for histological analysis. To unmask antigens, we boiled 5-μm sections in Target Retrieval solution (Dako USA) in a pressure cooker. Ki-67 was stained as described in the manufacturer's protocol (Dako USA) with biotinylated secondary antibody to rat IgG (Dako USA). We used the ApopTag Apoptosis Detection Kit for TUNEL staining according to the manufacturer's protocol (Chemicon). Cleaved–caspase-3 staining was performed as described in the manufacturer's protocol (Cell Signaling Technology). *Dolichos biflorus* agglutinin (DBA) and *Lotus tetragonolobus* lectin (LTL) (Vector Laboratories) were used at a dilution of 1:100. Antibodies to aquaporin-2 and Tamm-Horsfall glycoprotein were gifts (see Acknowledgments) and were each used at a 1:500 dilution. Secondary antibody (Jackson ImmunoResearch Laboratories) conjugated to Cy3 was used at a 1:400 dilution. We captured images with a Nikon Eclipse E600 microscope and either a SPOT-RT monochromic (SPOT Diagnostic Instruments) or a Nikon DXM1200 digital camera.

Proliferation studies. Sections were scanned on an Olympus IX81 microscope with a Prior Proscan II controller and Hamamatsu EM-CCD C9100 digital camera and were analyzed with Slidebook Pro 4.1 software using the automated stitching function. We exported stitched images composed of Cy3 and DAPI captures as individual 16-bit channels in TIFF format. For sections too large to be assembled into one file (because of memory limitations), we performed two or three nonoverlapping scans instead. Individual TIFF files were opened in ImageJ 1.39a, and the nucleus-counter function of the WCIF plug-in was used to count the number of labeled nuclei (Cy3 for Ki-67–positive nuclei, DAPI for total number of nuclei). For each sample, we captured a set of 50–100 images at $\times 10$ magnification for analysis.

Statistical analyses. We calculated the statistical significance of differences in proliferation rates using the Mann-Whitney (**Table 1a**) or Kruskal-Wallis (**Table 1b,c**) nonparametric tests and considered a value of $P < 0.05$ significant.

Microarrays. We isolated total RNA from kidneys with the Qiagen RNA extraction kit. We determined RNA concentration by spectrophotometry (NanoDrop) and then used 10 μg of total RNA for each hybridization. We analyzed 16 kidneys of uninduced *Pkd1*$^{cond/cond}$; tamoxifen-Cre^{-} , *Pkd1*$^{cond/cond}$; tamoxifen-Cre^{+}, and ROSA26R^{+} mice (four samples from each time point: P11, P12, P14 and P15) with Mouse RefS equation 8 (8) Illumina Sentrix BeadChip microarray chips. The P11 and P14 animals were littermates, as were the P12 and P15 animals. Two samples from each time point were randomly selected for technical replication with the same platform. The results were analyzed with implementations provided by the open-source bioconductor project (http://www.bioconductor.org)[27]. Briefly, we used the $\log_2$ of expression values, followed by quantile normalization and linear model and empirical Bayes methods for differential gene-expression analysis[28]. The comparisons included (P11 and P12) versus (P14 and P15), (P11 and P14) versus (P12 and P15), and (P11 and P15) versus (P12 and P14). We considered genes with an *fdr*-adjusted *P*-value less than 1×10^{-3} in the first contrast, but not in the other two, as significantly different. Multidimensional scaling analysis was performed by using the correlation matrix of the expression values. Identification of overrepresented promoter *cis* elements was done with PRIMO (http://gastro.imbg.ku.dk/primoweb/)[29]. Gene ontological classification[9] of the differentially expressed genes was performed by using the DAVID Bioinformatics Database functional-annotation tools (http://david.abcc.ncifcrf.gov/)[30]. The microarray data have been deposited in the Gene Expression Omnibus maintained by the US National Center for Biotechnology Information (http://www.ncbi.nlm.nih.gov/geo/).

Accession numbers. Gene Expression Omnibus series GSE9167.

Note: Supplementary information is available on the Nature Medicine website.

ACKNOWLEDGMENTS

This work was supported by grants from the US National Institutes of Health (DK48006, DK51259) and the US National Kidney Foundation (L.F.M.). G.G.G. is the Irving Blum Scholar of the Johns Hopkins University School of Medicine. The authors wish to thank members of the Germino, Watnick, Montell, Qian and Sutters laboratories (Johns Hopkins University School of Medicine), A. Tousson (University of Alabama at Birmingham) and S. Kuo (Johns Hopkins University School of Medicine) for helpful advice, C. Cheadle (Johns Hopkins Bayview Medical Campus Genomics Core) for assistance with the microarray studies, and M. Knepper (US National Institutes of Health) and J. Hoyer (Children's Hospital of Philadelphia) for the antibodies to aquaporin-2 and Tamm-Horsfall glycoprotein, respectively.

AUTHOR CONTRIBUTIONS

K.P. designed and performed the experiments and contributed to the writing of the manuscript. L.F.M. assisted in the experimental design, helped to analyze the histopathology, performed the microarray analyses and assisted in the writing of the manuscript. M.A.G.-G. helped perform the experiments and contributed conceptually to the project. D.L.H. helped with the histopathology. G.G.G. directed the project and wrote the manuscript.

Published online at http://www.nature.com/naturemedicine
Reprints and permissions information is available online at http://npg.nature.com/reprintsandpermissions

1. Boucher, C. & Sandford, R. Autosomal dominant polycystic kidney disease (ADPKD, MIM 173900, *PKD1* and *PKD2* genes, protein products known as polycystin-1 and polycystin-2). *Eur. J. Hum. Genet.* **12**, 347–354 (2004).
2. Pretorius, D.H. *et al.* Diagnosis of autosomal dominant polycystic kidney disease *in utero* and in the young infant. *J. Ultrasound Med.* **6**, 249–255 (1987).
3. Piontek, K.B. *et al.* A functional floxed allele of *Pkd1* that can be conditionally inactivated *in vivo*. *J. Am. Soc. Nephrol.* **15**, 3035–3043 (2004).
4. Lu, W. *et al.* Perinatal lethality with kidney and pancreas defects in mice with a targetted *Pkd1* mutation. *Nat. Genet.* **17**, 179–181 (1997).
5. Bukanov, N.O., Smith, L.A., Klinger, K.W., Ledbetter, S.R. & Ibraghimov-Beskrovnaya, O. Long-lasting arrest of murine polycystic kidney disease with CDK inhibitor roscovitine. *Nature* **444**, 949–952 (2006).
6. Lanoix, J., D'Agati, V., Szabolcs, M. & Trudel, M. Dysregulation of cellular proliferation and apoptosis mediates human autosomal dominant polycystic kidney disease (ADPKD). *Oncogene* **13**, 1153–1160 (1996).
7. Woo, D. Apoptosis and loss of renal tissue in polycystic kidney diseases. *N. Engl. J. Med.* **333**, 18–25 (1995).
8. Ashburner, M. *et al.* Gene ontology: tool for the unification of biology. The Gene Ontology Consortium. *Nat. Genet.* **25**, 25–29 (2000).
9. Chotteau-Lelievre, A. *et al.* PEA3 transcription factors are expressed in tissues undergoing branching morphogenesis and promote formation of duct-like structures by mammary epithelial cells *in vitro*. *Dev. Biol.* **259**, 241–257 (2003).
10. Grantham, J.J., Geiser, J.L. & Evan, A.P. Cyst formation and growth in autosomal dominant polycystic kidney disease. *Kidney Int.* **31**, 1145–1152 (1987).
11. Nadasdy, T. *et al.* Proliferative activity of cyst epithelium in human renal cystic diseases. *J. Am. Soc. Nephrol.* **5**, 1462–1468 (1995).
12. Chang, M.Y. *et al.* Haploinsufficiency of *Pkd2* is associated with increased tubular cell proliferation and interstitial fibrosis in two murine *Pkd2* models. *Nephrol. Dial. Transplant.* **21**, 2078–2084 (2006).
13. Shillingford, J.M. *et al.* The mTOR pathway is regulated by polycystin-1, and its inhibition reverses renal cystogenesis in polycystic kidney disease. *Proc. Natl. Acad. Sci. USA* **103**, 5466–5471 (2006).
14. Sweeney, W.E. Jr. *et al.* Combination treatment of PKD utilizing dual inhibition of EGF-receptor activity and ligand bioavailability. *Kidney Int.* **64**, 1310–1319 (2003).
15. Muskhelishvili, L., Latendresse, J.R., Kodell, R.L. & Henderson, E.B. Evaluation of cell proliferation in rat tissues with BrdU, PCNA, Ki-67 (MIB-5) immunohistochemistry and *in situ* hybridization for histone mRNA. *J. Histochem. Cytochem.* **51**, 1681–1688 (2003).
16. Simons, M. *et al.* Inversin, the gene product mutated in nephronophthisis type II, functions as a molecular switch between Wnt signaling pathways. *Nat. Genet.* **37**, 537–543 (2005).
17. Fischer, E. *et al.* Defective planar cell polarity in polycystic kidney disease. *Nat. Genet.* **38**, 21–23 (2006).
18. Ciruna, B., Jenny, A., Lee, D., Mlodzik, M. & Schier, A.F. Planar cell polarity signalling couples cell division and morphogenesis during neurulation. *Nature* **439**, 220–224 (2006).
19. Torres, V.E. *et al.* Effective treatment of an orthologous model of autosomal dominant polycystic kidney disease. *Nat. Med.* **10**, 363–364 (2004).
20. Wu, G. *et al.* Somatic inactivation of *Pkd2* results in polycystic kidney disease. *Cell* **93**, 177–188 (1998).
21. Osathanondh, V. & Potter, E.L. Pathogenesis of polycystic kidneys. Historical Survey. *Arch. Pathol.* **77**, 459–465 (1964).
22. Heggo, O. A microdissection study of cystic disease of the kidneys in adults. *J. Pathol. Bacteriol.* **91**, 311–315 (1966).
23. Baert, L. Hereditary polycystic kidney disease (adult form): a microdissection study of two cases at an early stage of the disease. *Kidney Int.* **13**, 519–525 (1978).
24. Calvet, J.P. Injury and development in polycystic kidney disease. *Curr. Opin. Nephrol. Hypertens.* **3**, 340–348 (1994).
25. Nauli, S.M. *et al.* Polycystins 1 and 2 mediate mechanosensation in the primary cilium of kidney cells. *Nat. Genet.* **33**, 129–137 (2003).
26. Davenport, J.R. *et al.* Disruption of intraflagellar transport in adult mice leads to obesity and slow-onset cystic kidney disease. *Curr. Biol.* **17**, 1586–1594 (2007).
27. Gentleman, R.C. *et al.* Bioconductor: open software development for computational biology and bioinformatics. *Genome Biol.* **5**, R80 (2004).
28. Smyth, G. LIMMA: linear models for microarray data. in *Bioinformatics and Computational Biology Solutions Using R and Bioconductor* (Eds. Gentleman, R., Carey, V.J., Huber, W., Irizarry, R.A., Dudoit, S.) 397–420 (Springer, New York City, 2005).
29. Stegmann, A. *et al.* Metabolome, transcriptome, and bioinformatic cis-element analyses point to HNF-4 as a central regulator of gene expression during enterocyte differentiation. *Physiol. Genomics* **27**, 141–155 (2006).
30. Dennis, G., Jr. *et al.* DAVID: database for annotation, visualization, and integrated discovery. *Genome Biol.* **4**, P3 (2003).